INTERNATIONAL JOURNAL OF
NUMERICAL ANALYSIS AND MODELING
Volume 21, Number 1, Pages 1–19

doi: 10.4208/ijnam2024-1001

A PARALLEL ITERATIVE PROCEDURE FOR WEAK GALERKIN METHODS FOR SECOND ORDER ELLIPTIC PROBLEMS

CHUNMEI WANG*, JUNPING WANG, AND SHANGYOU ZHANG

Abstract. A parallelizable iterative procedure based on domain decomposition is presented and analyzed for weak Galerkin finite element methods for second order elliptic equations. The convergence analysis is established for the decomposition of the domain into individual elements associated to the weak Galerkin methods or into larger subdomains. A series of numerical tests are illustrated to verify the theory developed in this paper.

Key words. Weak Galerkin, finite element methods, elliptic equation, parallelizable iterative, domain decomposition.

1. Introduction

This paper is concerned with an iterative procedure related to domain decomposition techniques based on the use of subdomains as small as individual elements for weak Galerkin (WG) methods for second order elliptic equations in $\mathbb{R}^d (d = 2, 3)$. For simplicity, we consider the second order elliptic problem with a Dirichlet boundary condition

$$\begin{aligned} -\nabla \cdot (a\nabla u) + cu &= f, \qquad \text{in } \Omega \subset \mathbb{R}^d, \\ u &= g, \qquad \text{on } \partial\Omega, \end{aligned} \tag{1}$$

where $d = 2, 3$. Assume the coefficients $a(x)$ and $c(x)$ satisfy

$$0 < a_0 \le a(x) \le a_1 < \infty, \quad 0 \le c(x) \le c_1 < \infty,$$

and are sufficiently regular so that the existence and uniqueness of a solution of (1) in $H^s(\Omega)$ hold true for some $s > 1$ for reasonable f and g. A weak formulation for the model problem (1) reads as follows: Find $u \in H^1(\Omega)$ such that $u = g$ on $\partial\Omega$, satisfying

$$(a\nabla u, \nabla v) + (cu, v) = (f, v) \qquad \forall v \in H_0^1(\Omega). \tag{2}$$

The WG finite element method is emerging as a new and efficient numerical method for solving partial differential equations (PDEs). The idea of WG method was first proposed by Wang and Ye for solving second order elliptic equations in 2011 [33]. This method was subsequently developed for various PDEs, see [15, 16, 18, 19, 20, 31, 27, 30, 28, 26, 31, 33, 34, 17, 35, 36, 27, 29, 32]. Due to the large size of the computational problem, it is necessary and crucial to design efficient and parallelizable iterative algorithms for the WG scheme. There have been some iterative algorithms designed for the WG methods along the line of domain decompositions [23, 5, 22, 21, 14]. Our iterative procedure is motivated by Despres [6] for a Helmholz problem and another Helmholz-like problem related to Maxwell's equations by Despres [7, 8]. It should be noted that the convergence in [6, 7, 8]

Received by the editors on January 30, 2023 and, accepted on August 21, 2023.
2000 *Mathematics Subject Classification.* Primary, 65N30, 65N15, 65N12, 74N20; Secondary, 35B45, 35J50, 35J35.
*Corresponding author.

were established for the differential problems in strong form where numerical results were presented to validate the iterative procedures for the discrete case. Douglas et al. [9] introduced a parallel iterative procedure for the second order partial differential equations by using the mixed finite element methods. The goal of this paper is to extend the result of Douglas into weak Galerkin finite element methods. In particular, based on the features of weak Galerkin methods, the iterative procedure developed in this paper can be very naturally and easily implemented on a massively parallel computer by assigning each subdomain to its own processor.

The paper is organized as follows. In Section 2, we briefly review the weak differential operators and their discrete analogies. In Section 3, we describe the WG method for the model problem (1). In Section 4, we introduce domain decompositions and derive a hybridized formulation for the WG method. In Section 5, we present a parallel iterative procedure for the WG finite element method. In Section 6, we establish a convergence analysis for the parallel iterative scheme. Finally in Section 7, we report several numerical results to verify our convergence theory.

2. Weak Differential Operators

The primary differential operator in the weak formulation (2) for the second order elliptic problem (1) is the gradient operator ∇, for which a discrete weak version has been introduced in [34]. For completeness, let us briefly review the definition as follows.

Let T be a polygonal or polyhedral domain with boundary ∂T. A weak function on T refers to $v = \{v_0, v_b\}$ where $v_0 \in L^2(T)$ and $v_b \in L^2(\partial T)$ represent the values of v in the interior and on the boundary of T respectively. Note that v_b may not necessarily be the trace of v_0 on ∂T. Denote by $W(T)$ the local space of weak functions on T; i.e.,

$$W(T) = \{v = \{v_0, v_b\} : v_0 \in L^2(T), v_b \in L^2(\partial T)\}.$$

The weak gradient of $v \in W(T)$, denoted by $\nabla_w v$, is defined as a linear functional on $[H^1(T)]^d$ such that

$$(\nabla_w v, \mathbf{w})_T = -(v_0, \nabla \cdot \mathbf{w})_T + \langle v_b, \mathbf{w} \cdot \mathbf{n}\rangle_{\partial T} \qquad \forall \mathbf{w} \in [H^1(T)]^d.$$

Denote by $P_r(T)$ the space of all polynomials on T with total degree r and/or less. A discrete version of $\nabla_w v$ for $v \in W(T)$, denoted by $\nabla_{w,r,T} v$, is defined as a unique polynomial vector in $[P_r(T)]^d$ satisfying

$$(\nabla_{w,r,T} v, \mathbf{w})_T = -(v_0, \nabla \cdot \mathbf{w})_T + \langle v_b, \mathbf{w} \cdot \mathbf{n}\rangle_{\partial T}, \quad \forall \mathbf{w} \in [P_r(T)]^d. \tag{3}$$

3. Weak Galerkin Algorithm

Let $\mathcal{T}_h$ be a finite element partition of the domain Ω consisting of polygons or polyhedra that are shape-regular [34]. Denote by $\mathcal{E}_h$ the set of all edges or flat faces in $\mathcal{T}_h$ and $\mathcal{E}_h^0 = \mathcal{E}_h \setminus \partial\Omega$ the set of all interior edges or flat faces. Denote by h_T the meshsize of $T \in \mathcal{T}_h$ and $h = \max_{T\in\mathcal{T}_h} h_T$ the meshsize for the partition $\mathcal{T}_h$.

For any given integer $k \geq 1$, denote by $W_k(T)$ the local discrete space of the weak functions given by

$$W_k(T) = \{\{v_0, v_b\} : v_0 \in P_k(T), v_b \in P_{k-1}(e), e \subset \partial T\}. \tag{4}$$

Patching the local discrete space $W_k(T)$ with a single value on the element interface yields the global finite element space; i.e.,

$$W_h = \{v = \{v_0, v_b\} : \ v|_T \in W_k(T), v_b \text{ is single-valued on } e \subset \mathcal{E}_h^0, T \in \mathcal{T}_h\}.$$

Denote by W_h^g and W_h^0 the subspaces of W_h with non-homogeneous and homogeneous boundary values; i.e.,

$$W_h^g = \{\{v_0, v_b\} \in W_h : \ v_b|_e = Q_b g, e \subset \partial\Omega\},$$
$$W_h^0 = \{\{v_0, v_b\} \in W_h : \ v_b|_e = 0, e \subset \partial\Omega\},$$

where Q_b is the L^2 projection onto the space $P_{k-1}(e)$.

For $v \in W_h$, denote by $\nabla_w v$ the discrete weak action $\nabla_{w,k-1,T} v$ computed by using (3) on each element T; i.e.,

$$(\nabla_w v)|_T = \nabla_{w,k-1,T}(v|_T). \tag{5}$$

Next, we introduce the following bilinear forms in $W_h \times W_h$:

$$s(u,v) = \sum_{T\in\mathcal{T}_h} s_T(u,v), \tag{6}$$

$$a(u,v) = \sum_{T\in\mathcal{T}_h} a_T(u,v), \tag{7}$$

where

$$\begin{aligned} s_T(u,v) &= h_T^{-1}\langle Q_b u_0 - u_b, Q_b v_0 - v_b\rangle_{\partial T}, \\ a_T(u,v) &= (a\nabla_w u, \nabla_w v)_T + (cu_0, v_0)_T. \end{aligned}$$

The weak Galerkin finite element scheme for the second order problem (1) based on the variational formulation (2) can be stated as follows:

Algorithm 3.1. *Find $\bar{u}_h \in W_h^g$, such that*

$$s(\bar{u}_h, v) + a(\bar{u}_h, v) = (f, v_0) \qquad \forall v \in W_h^0. \tag{8}$$

4. Weak Galerkin based on Domain Decompositions

Let $\{\Omega_j : j = 1, \cdots, M\}$ be a partition of Ω such that

$$\overline{\Omega} = \bigcup_{j=1}^{M} \overline{\Omega}_j, \qquad \Omega_j \cap \Omega_k = \emptyset, j \neq k. \tag{9}$$

In practice, with the exception of a few Ω_j's along $\partial\Omega$, each Ω_j is convex with a piecewise-smooth boundary. We introduce, cf. Figure 1,

$$\Gamma = \partial\Omega, \qquad \Gamma_j = \Gamma \cap \partial\Omega_j, \qquad \Gamma_{jk} = \Gamma_{kj} = \partial\Omega_j \cap \partial\Omega_k.$$

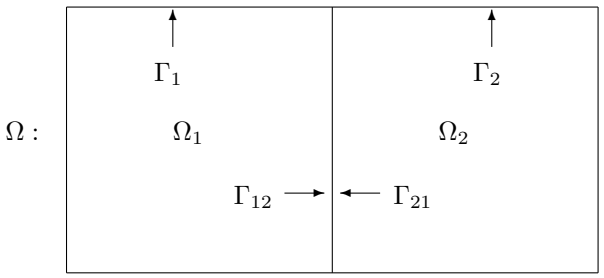

FIGURE 1. A domain is subdivided into two subdomains, $M = 2$.

Assume that the edges/faces of the elements in $\mathcal{T}_h$ align with the interface $I_f = \bigcup_{j,k=1}^{M} \Gamma_{jk}$. The partition $\mathcal{T}_h$ can be grouped into M sets of elements denoted by $\mathcal{T}_h^i = \mathcal{T}_h \cap \Omega_i$, so that each $\mathcal{T}_h^i$ provides a finite element partition for the subdomain

Ω_i for $i = 1, \cdots, M$. The intersection of the partitions $\mathcal{T}_h^j$ and $\mathcal{T}_h^k$ also introduces a finite element partition for the interface Γ_{jk}, denoted by Γ_{jk}^h.

Let us introduce the Lagrange multipliers on the edge Γ_{jk} as seen from Ω_j as follows

$$\Lambda_{jk} = \{\lambda_{jk} : \lambda_{jk} \in P_{k-1}(\Gamma_{jk} \cap \Omega_j), \Gamma_{jk} \neq \emptyset \text{ is of dimension } d-1, \forall j, k = 1, \cdots, M\}.$$

Note that there are two copies of $P_{k-1}(e)$ assigned to the interface Γ_{jk} as seen from Ω_j and Ω_k respectively; i.e., Λ_{jk} and Λ_{kj}. Note that the Lagrangian space Λ_{jk} is defined only on $d-1$ dimensional interfaces $\Gamma_{jk} \subset \mathbb{R}^{d-1}$.

Define, for $j = 1, \cdots, M$, the finite element space on each subdomain Ω_j:

$$\begin{aligned} W_h(\Omega_j) &= \{v|_{\Omega_j} : \ v \in W_h\}, \\ W_h^0(\Omega_j) &= \{v \in W_h(\Omega_j) : v|_{\Gamma_j} = 0\}. \end{aligned}$$

The weak Galerkin finite element method (8) restricted in the subdomain Ω_j ($j = 1, \cdots, M$) is as follows: Find $u_j = \{u_{j,0}, u_{j,b}\} \in W_h(\Omega_j)$, such that $u_{j,b} = Q_b g$ on Γ_j, $\lambda_{jk} \in \Lambda_{jk}$, $j, k = 1, \cdots, M$,

$$\begin{cases} (a\nabla_w u_j, \nabla_w v_j)_{\Omega_j} + s_j(u_j, v_j) - \sum_{k=1}^{M} \langle \lambda_{jk}, v_{j,b} \rangle_{\Gamma_{jk}} \\ + (cu_{j,0}, v_{j,0})_{\Omega_j} = (f, v_{j,0})_{\Omega_j}, \qquad \forall v_j \in W_h^0(\Omega_j), \\ \sum_{k=1}^{M} \langle \mu, [\![u_b]\!]_{\Gamma_{jk}} \rangle_{\Gamma_{jk}} = 0, \qquad \forall \mu \in \Lambda_{jk}, \\ \lambda_{jk} + \lambda_{kj} = 0, \qquad \text{on } \Gamma_{jk}, \end{cases} \tag{10}$$

where $(\cdot,\cdot)_{\Omega_j} = \sum_{T \in \mathcal{T}_h^j} (\cdot,\cdot)_T$, $s_j(u_j, v_j) = \sum_{T \in \mathcal{T}_h^j} s_T(u, v)$, and $[\![u_b]\!]_{\Gamma_{jk}}$ is the jump of u_b on Γ_{jk} defined as follows:

$$[\![u_b]\!]_{\Gamma_{jk}} = u_{b,j}|_{\Gamma_{jk} \cap \Omega_j} - u_{b,k}|_{\Gamma_{kj} \cap \Omega_k}, \tag{11}$$

where $u_{b,j}|_{\Gamma_{jk} \cap \Omega_j}$ and $u_{b,k}|_{\Gamma_{kj} \cap \Omega_k}$ represent the values of u_b on Γ_{jk} as seen from Ω_j and Ω_k respectively.

Lemma 4.1. *Let $u_j = \{u_{j,0}, u_{j,b}\} \in W_h(\Omega_j)$ and $\lambda_{jk} \in \Lambda_{jk}$ be the solution of the algorithm (10). Then, we have $[\![u_b]\!]_{\Gamma_{jk}} = 0$ for $j, k = 1, \cdots, M$, so that $u_h|_{\Omega_j} = u_j$ is a function in the finite element space W_h. Furthermore, this function u_h satisfies the WG scheme (8). In other words, we have $u_h \equiv \bar{u}_h$.*

Proof. By letting $\mu = [\![u_b]\!]_{\Gamma_{jk}} \in \Lambda_{jk}$ and then using the second equation in (10) we arrive at

$$0 = \sum_{j,k=1}^{M} \int_{\Gamma_{jk}} [\![u_b]\!]_{\Gamma_{jk}}^2 ds,$$

which implies that $[\![u_b]\!]_{\Gamma_{jk}} = 0$ for $j, k = 1, \cdots, M$.

Next, by restricting $v \in W_h^0$ in the first equation in (10) and using the fact that $\lambda_{jk} + \lambda_{kj} = 0$ we have

$$\sum_{j,k=1}^{M} \langle \lambda_{jk}, v_b \rangle_{\Gamma_{jk}} = 0,$$

which leads to

$$a(u_h, v) + s(u_h, v) = (f, v_0) \qquad \forall v \in W_h^0.$$

It follows from $u_{j,b} = Q_b g$ on Γ_j that $u_h \in W_h^g$, which together with the last equation shows that u_h is a solution of the WG scheme (8). Finally, from the solution uniqueness for (8) we have $u_h \equiv \bar{u}_h$. This completes the proof. □

5. A Parallel Iterative Scheme

A parallel iterative scheme for the weak Galerkin finite element method can be designed by using the equivalent numerical scheme (10). The motivation of the iterative procedure comes from the observation that, in (10), the following consistency conditions

$$\begin{aligned} u_{j,b} &= u_{k,b}, \qquad \text{on } \Gamma_{jk}, \\ \lambda_{jk} &= -\lambda_{kj}, \qquad \text{on } \Gamma_{jk}, \end{aligned} \tag{12}$$

are equivalent to

$$\begin{aligned} \beta u_{j,b} + \lambda_{jk} &= \beta u_{k,b} - \lambda_{kj}, \qquad \text{on } \Gamma_{jk}, \\ \beta u_{k,b} + \lambda_{kj} &= \beta u_{j,b} - \lambda_{jk}, \qquad \text{on } \Gamma_{kj}, \end{aligned} \tag{13}$$

for any non-zero function β on $\bigcup_{j,k=1}^{M} \Gamma_{jk}$. This gives rise to

$$\langle \lambda_{jk}, v_{j,b} \rangle_{\Gamma_{jk}} = \langle \beta(u_{k,b} - u_{j,b}) - \lambda_{kj}, v_{j,b} \rangle_{\Gamma_{jk}}, \tag{14}$$

where $v_j = \{v_{j,0}, v_{j,b}\} \in W_h(\Omega_j)$. The use of the equation (14) in the numerical scheme (10) is a critical step in the design of the following parallel iterative procedure.

Starting from any initial guess $u_j^{(0)} = \{u_{j,0}^{(0)}, u_{j,b}^{(0)}\} \in W_h(\Omega_j)$ with $u_{j,b}^{(0)} = Q_b g$ on Γ_j, $\lambda_{jk}^{(0)} \in \Lambda_{jk}$ and $\lambda_{kj}^{(0)} \in \Lambda_{kj}$, we solve for $u_j^{(n)} = \{u_{j,0}^{(n)}, u_{j,b}^{(n)}\} \in W_h(\Omega_j)$, $\lambda_{jk}^{(n)} \in \Lambda_{jk}$, and $\lambda_{kj}^{(n)} \in \Lambda_{kj}$ such that $u_{j,b}^{(n)} = Q_b g$ on Γ_j and satisfying the following system of linear equations

$$\begin{cases} (a\nabla_w u_j^{(n)}, \nabla_w v_j)_{\Omega_j} + s_j(u_j^{(n)}, v_j) + \displaystyle\sum_{k=1}^{M} \langle \beta u_{j,b}^{(n)}, v_{j,b} \rangle_{\Gamma_{jk}} + (c u_{j,0}^{(n)}, v_{j,0})_{\Omega_j} \\ = \displaystyle\sum_{k=1}^{M} \langle \beta u_{k,b}^{(n-1)} - \lambda_{kj}^{(n-1)}, v_{j,b} \rangle_{\Gamma_{jk}} + (f, v_{j,0})_{\Omega_j} \quad \forall v_j \in W_h^0(\Omega_j), \\ \lambda_{jk}^{(n)} = \beta(u_{k,b}^{(n-1)} - u_{j,b}^{(n)}) - \lambda_{kj}^{(n-1)}. \end{cases} \tag{15}$$

6. Convergence

Let us establish the convergence for the iteration procedure defined in (15). To this end, for $e = \{e_j : \ e_j \in W_h(\Omega_j)\}$ and $\mu = \{\mu_{jk} : \ \mu_{jk} \in \Lambda_{jk}\}$, denote by

$$\begin{aligned} (a\nabla_w e, \nabla_w e) &= \sum_{j=1}^{M} (a\nabla_w e_j, \nabla_w e_j)_{\Omega_j}, \\ (ce_0, e_0) &= \sum_{j=1}^{M} (ce_{j,0}, e_{j,0})_{\Omega_j}, \\ s(e,e) &= \sum_{j=1}^{M} s_j(e_j, e_j). \end{aligned}$$

Moreover, denote by

$$\begin{aligned} E(\{e,\mu\}) &= \sum_{j=1}^{M}\beta^2|e_{j,b}|^2_{0,B_j}+\sum_{j,k=1}^{M}|\mu_{jk}|^2_{0,\Gamma_{jk}} \\ &\quad +2\beta\{(a\nabla_w e,\nabla_w e)+s(e,e)+(ce_0,e_0)\}, \end{aligned}$$

where $B_j=\partial\Omega_j\setminus\Gamma_j$.

Let $\{u_j,\lambda_{jk}\}$ be the solution of the domain-decomposition-based numerical scheme (10). We define the error functions:

$$e_j^{(n)}=u_j-u_j^{(n)},\qquad \mu_{jk}=\lambda_{jk}-\lambda_{jk}^{(n)},\qquad \mu_{kj}=\lambda_{kj}-\lambda_{kj}^{(n)}. \tag{16}$$

The error equations for the iterative procedure (15) can be written in the form:

$$\begin{cases} (a\nabla_w e_j^{(n)},\nabla_w v_j)_{\Omega_j}+s_j(e_j^{(n)},v_j)-\sum_{k=1}^{M}\langle\mu_{jk}^{(n)},v_{j,b}\rangle_{\Gamma_{jk}} \\ \quad +(ce_{j,0}^{(n)},v_{j,0})_{\Omega_j}=0,\qquad \forall v_j\in W_h(\Omega_j), \\ \mu_{jk}^{(n)}=\beta(e_{k,b}^{(n-1)}-e_{j,b}^{(n)})-\mu_{kj}^{(n-1)}, \end{cases} \tag{17}$$

Lemma 6.1. *Let $E^{(n)}=E(\{e^{(n)},\mu^{(n)}\})$. The following identities hold true*

$$\begin{aligned} &E^{(n-1)}-E^{(n)} \\ =&4\beta\{(a\nabla_w e^{(n-1)},\nabla_w e^{(n-1)})+s(e^{(n-1)},e^{(n-1)})+(ce_0^{(n-1)},e_0^{(n-1)})\}, \end{aligned} \tag{18}$$

where

$$\begin{aligned} E^{(n)} =&\beta^2|e_{j,b}^{(n)}|^2_{0,B_j}+\sum_{k=1}^{M}|\mu_{jk}^{(n)}|^2_{0,\Gamma_{jk}} \\ &+2\beta\{(a\nabla_w e_j^{(n)},\nabla_w e_j^{(n)})_{\Omega_j}+s_j(e_j^{(n)},e_j^{(n)})+(ce_{j,0}^{(n)},e_{j,0}^{(n)})_{\Omega_j}\}. \end{aligned} \tag{19}$$

Proof. Note that $e_{j,b}^{(n)}=0$ on Γ_j. By letting $v_j=e_j^{(n)}$ in the first equation of (17) we obtain

$$(a\nabla_w e_j^{(n)},\nabla_w e_j^{(n)})_{\Omega_j}+s_j(e_j^{(n)},e_j^{(n)})-\sum_{k=1}^{M}\langle\mu_{jk}^{(n)},e_{j,b}^{(n)}\rangle_{\Gamma_{jk}}+(ce_{j,0}^{(n)},e_{j,0}^{(n)})_{\Omega_j}=0. \tag{20}$$

From (20) we have

$$\begin{aligned} E^{(n)} =&\sum_{k=1}^{M}|\beta e_{j,b}^{(n)}+\mu_{jk}^{(n)}|^2_{0,\Gamma_{jk}} \\ =&\beta^2|e_{j,b}^{(n)}|^2_{0,B_j}+\sum_{k=1}^{M}|\mu_{jk}^{(n)}|^2_{0,\Gamma_{jk}}+2\beta\sum_{k=1}^{M}\langle e_{j,b}^{(n)},\mu_{jk}^{(n)}\rangle_{\Gamma_{jk}} \\ =&\beta^2|e_{j,b}^{(n)}|^2_{0,B_j}+\sum_{k=1}^{M}|\mu_{jk}^{(n)}|^2_{0,\Gamma_{jk}} \\ &+2\beta\{(a\nabla_w e_j^{(n)},\nabla_w e_j^{(n)})_{\Omega_j}+s_j(e_j^{(n)},e_j^{(n)})+(ce_{j,0}^{(n)},e_{j,0}^{(n)})_{\Omega_j}\}, \end{aligned}$$

which verifies the identify (19).

Next, from the second equation in (17) we have

$$
\begin{aligned}
E^{(n)} =& \sum_{j=1}^{M}\sum_{k=1}^{M} |\beta e_{j,b}^{(n)} + \mu_{jk}^{(n)}|_{0,\Gamma_{jk}}^2 \\
=& \sum_{k=1}^{M}\sum_{j=1}^{M} |\beta e_{k,b}^{(n-1)} - \mu_{kj}^{(n-1)}|_{0,\Gamma_{kj}}^2 \\
=& E^{(n-1)} - 4\beta \sum_{k=1}^{M} \{(a\nabla_w e_k^{(n-1)}, \nabla_w e_k^{(n-1)})_{\Omega_k} + s_k(e_k^{(n-1)}, e_k^{(n-1)}) \\
&+ (ce_{k,0}^{(n-1)}, e_{k,0}^{(n-1)})_{\Omega_k}\},
\end{aligned} \tag{21}
$$

which leads to the identity (18). □

Remark 6.1. *By* (18) *of Lemme 6.1, as the right-hand side is non-negative,* $E^{(n)}$ *is a non-increasing sequence. Because* $E^{(n)}$ *is non-negative and non-increasing, it is bounded, and one of its three non-negative parts,* $|e_{j,b}^{(n)}|_{0,B_j}^2$*, is also bounded.*

The rest of this sections is concerned with two technical results that support the convergence analysis for the parallel iterative procedure.

Lemma 6.2. *There exists* $C_1 > 0$ *and* $C_2 > 0$ *such that*

$$
\begin{aligned}
C_1((\nabla v_0, \nabla v_0)_{\Omega_j} + s_j(v,v)) \le (\nabla_w v, \nabla_w v)_{\Omega_j} + s_j(v,v) \\
\le C_2((\nabla v_0, \nabla v_0) + s_j(v,v))
\end{aligned}
$$

for any $v \in W_h(\Omega_j)$.

Proof. For each $T \in \mathcal{T}_h^j$, using (3) and the usual integration by parts yields

$$
\begin{aligned}
(\nabla_w v, \mathbf{w})_T =& -(v_0, \nabla\cdot\mathbf{w})_T + \langle v_b, \mathbf{w}\cdot\mathbf{n}\rangle_{\partial T} \\
=& (\nabla v_0, \mathbf{w})_T + \langle v_b - Q_b v_0, \mathbf{w}\cdot\mathbf{n}\rangle_{\partial T}.
\end{aligned}
$$

Now from the Cauchy-Schwarz inequality and the trace inequality we obtain

$$
\begin{aligned}
\|\nabla_w v\|_T \le& \frac{\|\nabla v_0\|_T\|\mathbf{w}\|_T + \|Q_b v_0 - v_b\|_{\partial T}\|\mathbf{w}\cdot\mathbf{n}\|_{\partial T}}{\|\mathbf{w}\|_T} \\
\le& C_2 \frac{\|\nabla v_0\|_T\|\mathbf{w}\|_T + \|Q_b v_0 - v_b\|_{\partial T} h_T^{-\frac{1}{2}}\|\mathbf{w}\|_T}{\|\mathbf{w}\|_T} \\
\le& C_2(\|\nabla v_0\|_T + h_T^{-\frac{1}{2}}\|Q_b v_0 - v_b\|_{\partial T}).
\end{aligned}
$$

Summing over all $T \in \mathcal{T}_h^j$ gives rise to the upper-bound estimate of $(\nabla_w v, \nabla_w v)_{\Omega_j} + s_j(v,v)$. The lower-bound estimate of $(\nabla_w v, \nabla_w v)_{\Omega_j} + s_j(v,v)$ can be established analogously. This completes the proof of the lemma. □

For $v_j = \{v_{j,0}, v_{j,b}\} \in W_h(\Omega_j)$, we define a semi-norm by setting

$$
|\!|\!| v_j |\!|\!|_{1,\Omega_j}^2 = \sum_{T\in\mathcal{T}_h^j} (a\nabla v_{j,0}, \nabla v_{j,0})_T + s_j(v_j, v_j) + \|v_{j,b}\|_{\partial\Omega_j}^2. \tag{22}
$$

Lemma 6.3. *The semi-norm* $|\!|\!|\cdot|\!|\!|_{1,\Omega_j}$ *defined in* (22) *is a norm in* $W_h(\Omega_j)$.

Proof. It suffices to verify the positivity property for $|\!|\!|\cdot|\!|\!|_{1,\Omega_j}$. To this end, assume $|\!|\!| v_j |\!|\!|_{1,\Omega_j} = 0$ for a weak function $v = \{v_{j,0}, v_{j,b}\} \in W_h(\Omega_j)$. It follows that $\nabla v_{j,0} = 0$ on each $T \in \mathcal{T}_h$, $Q_b v_{j,0} = v_{j,b}$ on each ∂T, and $v_{j,b} = 0$ on $\partial\Omega_j$. Therefore, we have $v_{j,0} = const$ on each $T \in \mathcal{T}_h^j$. Using $Q_b v_{j,0} = v_b$ on ∂T, we have $v_{j,0} = const$ in the

subdomain Ω_j. Using $v_{j,b}=0$ on $\partial\Omega_j$ and $Q_b v_{j,0}=v_{j,b}$ on ∂T, we obtain $v_{j,0}=0$ in Ω_j. Again from $Q_b v_{j,0}=v_{j,b}$ on ∂T we have $v_{j,b}=0$ in Ω_j. This completes the proof of the lemma. □

Theorem 6.1. *Let* $\{u_j^{(n)},\lambda_{jk}^{(n)}\}$ *be the solution of the iterative scheme* (15) *and* $\{e_j^{(n)},\mu_{jk}^{(n)}\}$ *be the error functions defined in* (16) *for the numerical scheme* (10). *For any* $\beta>0$, *the following convergence holds true:*

$$u_j^{(n)}\to u_j, \tag{23}$$

$$\lambda_{jk}^{(n)}\to \lambda_{jk} \tag{24}$$

as $n\to\infty$.

Proof. Note that, from Lemma 6.1, $\{E^{(n)}\}$ is a non-increasing sequence of non-negative numbers. Thus, we have, by summing (18),

$$\begin{aligned}&\sum_{n=0}^{\infty}\{(a\nabla_w e^{(n)},\nabla_w e^{(n)})+s(e^{(n)},e^{(n)})+(ce_0^{(n)},e_0^{(n)})\}\\ &=E^{(0)}-\lim_{n\to\infty}E^{(n)}<\infty.\end{aligned}$$

It implies

$$(a\nabla_w e^{(n)},\nabla_w e^{(n)})+s(e^{(n)},e^{(n)})+(ce_0^{(n)},e_0^{(n)})\to 0. \tag{25}$$

If $c>0$, the left-hand side of (25) is a coercive bilinear form, which implies $e^{(n)}\to 0$ as $n\to\infty$. For the case of $c=0$, the above argument would not go through so that new approaches are necessary. The rest of the proof assumes the general case of $c\geq 0$.

For $\mu^{(n)}=\{\mu_{jk}^{(n)}\}$, we construct $v^*=\{v_j^*\}$, where $v_j^*\in W_h(\Omega_j)$ assumes the value of $\mu_{jk}^{(n)}$ on Γ_{jk} and zero otherwise. It is easy to show that

$$\|\nabla_w v_j^*\|_{\Omega_j}^2+s_j(v_j^*,v_j^*)\leq Ch^{-1}\sum_{k=1}^{M}\|\mu_{jk}^{(n)}\|_{\Gamma_{jk}}^2. \tag{26}$$

Substituting v_j by v_j^* in (17) yields

$$(a\nabla_w e_j^{(n)},\nabla_w v_j^*)_{\Omega_j}+s_j(e_j^{(n)},v_j^*)-\sum_{k=1}^{M}\|\mu_{jk}^{(n)}\|_{\Gamma_{jk}}^2=0. \tag{27}$$

Hence,

$$\begin{aligned}\sum_{k=1}^{M}\|\mu_{jk}^{(n)}\|_{\Gamma_{jk}}^2=&(a\nabla_w e_j^{(n)},\nabla_w v_j^*)_{\Omega_j}+s_j(e_j^{(n)},v_j^*)\\ \leq&C(a\nabla_w e_j^{(n)},\nabla_w e_j^{(n)})_{\Omega_j}^{1/2}\|\nabla_w v_j^*\|_{\Omega_j}+s_j(e_j^{(n)},e_j^{(n)})^{1/2}s_j(v_j^*,v_j^*)^{1/2}.\end{aligned}$$

Using the estimate (26) in the above inequality gives

$$\begin{aligned}\sum_{k=1}^{M}\|\mu_{jk}^{(n)}\|_{\Gamma_{jk}}^2=&(a\nabla_w e_j^{(n)},\nabla_w v_j^*)_{\Omega_j}+s_j(e_j^{(n)},v_j^*)\\ \leq&Ch^{-1}\{(a\nabla_w e_j^{(n)},\nabla_w e_j^{(n)})+s_j(e_j^{(n)},e_j^{(n)})\}.\end{aligned}$$

It follows that $\sum_{j,k=1}^{M}\|\mu_{jk}^{(n)}\|_{\Gamma_{jk}}^2\to 0$ as $n\to\infty$, which asserts the convergence for the Lagrangian multiplier $\lambda_{jk}^{(n)}$.

To prove the convergence of $u_j^{(n)}$, we note from (19) that $\{e_{j,b}^{(n)}\}$ is a bounded sequence in $L^2(B_j)$, and hence from Lemma 6.2, $\{e_j^{(n)}\}$ is a bounded sequence with respect to the norm $|||\cdot|||_{1,\Omega_j}$. It follows that $\{e_j^{(n)}\}$ must have a convergent subsequence. Without loss of generality, we may assume that $\{e_j^{(n)}\}$ is convergent so that

$$e_j^{(n)} \to e_j^* \quad \text{as } n \to \infty.$$

By passing to the limit of $n \to \infty$ and using the face that $\mu_{jk}^{(n)} \to 0$, from (17) we obtain the following equations:

$$\begin{aligned} &(a\nabla_w e_j^*, \nabla_w v_j)_{\Omega_j} + s_j(e_j^*, v_j) + (ce_{j,0}^*, v_{j,0})_{\Omega_j} = 0, \qquad \forall v_j \in W_h(\Omega_j), \\ &e_{j,b}^* = e_{k,b}^*, \quad \text{on } \Gamma_{jk}, \end{aligned} \tag{28}$$

which implies that $e_j^* \equiv 0$ for $j = 1, \cdots, M$. This completes the proof of the theorem. □

7. Numerical Experiments

In this section, we shall report some numerical results to demonstrate the performance of the iterative procedure for the weak Galerkin finite element method (8) for the second order elliptic model problem (1).

We only test smooth problems. For problems with heterogeneous permeability coefficients $a(x, y)$, such as the test problems in [12, 13, 24], it is not clear how the method in this paper will perform computationally. In order to have a reliable approximation, one may have to match the interface coefficient jump with the mesh lines, or to use carefully designed multiscale finite element spaces, for these non-smooth problems.

7.1. Test Example 1. The configuration of the test is set up as follows: the coefficients are $a(x, y) = 2 - x(1 - x)$ and $c = 1$; the exact solution is

$$u(x, y) = 2^6 x^2(1 - x)^2 y^2(1 - y)^2; \tag{29}$$

and the domain is $\Omega = (0, 1)^2$. Note that this corresponds to a homogeneous Dirichlet boundary value problem. The triangular grids shown as in Figures 2 and 3 are employed in the numerical tests. The 4-subdomain iterations and 16-subdomain iterations are computed respectively. The $\{P_k, P_{k-1}\}$ weak Galerkin finite elements are defined in (4) in all computational cases. The finite element equation in the computation is defined by (8). The iterative method for solving the finite element systems of equations is defined in (15). In the computation, the iteration stops when the iterative error reaches the truncation error.

In Tables 1-6, we list the computational results for the $\{P_k, P_{k-1}\}$ weak Galerkin finite element defined in (4) when the weak gradient is discretized by $[P_{k-1}(T)]^2$ defined in (5). Note that $Q_h u = \{Q_0 u, Q_b u\}$ where Q_0 is the element-wise L^2 projection to space $P_k(T)$ and Q_b is the edge-wise L^2 projection to $P_{k-1}(e)$.

In Table 1, we choose $\beta = 8$ and the $\{P_1, P_0\}$ WG finite element (4). We can see from Table 1 that we have an order two convergence in the L^2-norm and an order one convergence in the energy norm. We list the number of domain-decomposition iterations when the domain is subdivided into 4 subdomains and 16 subdomains respectively. In theory, the number of iterations may increase on higher level grids. However, the number of iterations appears to be steady when using 4 subdomains and 16 subdomains.

In Table 2, we employ the $\{P_2, P_1\}$ WG finite element (4) and $\beta = 8$. We can see from Table 2 that we have an order three convergence in the L^2-norm and an order

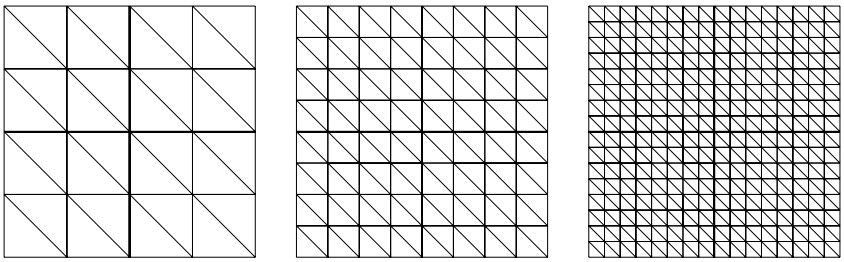

FIGURE 2. The level 2, 3 and 4 grids for the 4-subdomain computation.

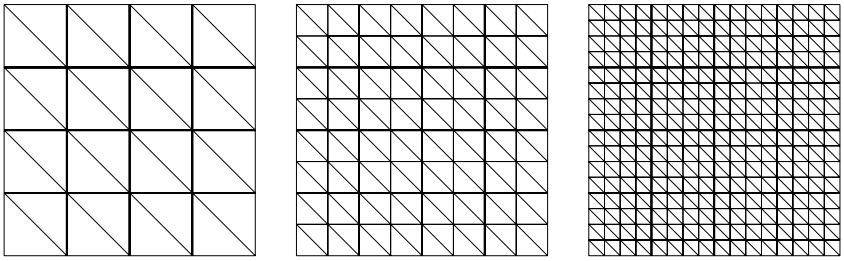

FIGURE 3. The level 2, 3 and 4 grids for the 16-subdomain computation.

TABLE 1. Error profile of $\{P_1, P_0\}$ solutions for (29) on Figures 2–3 grids.

Grid	$\|Q_0u - u_0\|_0$	rate	$\|\nabla_w(Q_hu - u_h)\|_0$	rate	# iteration
	The $\{P_1, P_0\}$ WG element (4), by 4-subdomain iteration.				
1	0.211E+00	0.0	0.614E-01	0.0	6
2	0.684E-01	1.6	0.181E+00	0.0	7
3	0.178E-01	1.9	0.110E+00	0.7	9
4	0.448E-02	2.0	0.579E-01	0.9	11
5	0.112E-02	2.0	0.293E-01	1.0	11
6	0.280E-03	2.0	0.147E-01	1.0	13
7	0.692E-04	2.0	0.734E-02	1.0	13
	The $\{P_1, P_0\}$ WG element (4), by 16-subdomain iteration.				
1	0.211E+00	0.0	0.614E-01	0.0	6
2	0.684E-01	1.6	0.181E+00	0.0	7
3	0.178E-01	1.9	0.110E+00	0.7	9
4	0.448E-02	2.0	0.578E-01	0.9	11
5	0.112E-02	2.0	0.292E-01	1.0	11
6	0.279E-03	2.0	0.147E-01	1.0	13
7	0.680E-04	2.0	0.734E-02	1.0	13

two convergence in the energy norm. In addition, the number of iterations needed for the 16-subdomain iteration is slightly higher than that of the 4-subdomain iteration.

In Table 3, $\beta = 8$ and $\{P_3, P_2\}$ weak Galerkin finite element are taken for the 4-subdomain and 16-subdomain iterations respectively. It can be seen from Table

TABLE 2. Error profile of $\{P_2, P_1\}$ solutions for (29) on Figures 2–3 grids.

Grid	$\|Q_0u - u_0\|_0$	rate	$\|\nabla_w(Q_hu - u_h)\|_0$	rate	# iteration
	The $\{P_2, P_1\}$ WG element (4), by 4-subdomain iteration.				
1	0.106E+00	0.0	0.110E+00	0.0	6
2	0.161E-01	2.7	0.351E-01	1.7	9
3	0.208E-02	3.0	0.102E-01	1.8	9
4	0.261E-03	3.0	0.274E-02	1.9	11
5	0.327E-04	3.0	0.708E-03	2.0	17
6	0.411E-05	3.0	0.183E-03	2.0	20
	The $\{P_2, P_1\}$ WG element (4), by 16-subdomain iteration.				
1	0.106E+00	0.0	0.110E+00	0.0	6
2	0.161E-01	2.7	0.352E-01	1.6	8
3	0.207E-02	3.0	0.103E-01	1.8	10
4	0.262E-03	3.0	0.275E-02	1.9	14
5	0.327E-04	3.0	0.709E-03	2.0	22
6	0.410E-05	3.0	0.182E-03	2.0	25

TABLE 3. Error profile of $\{P_3, P_2\}$ solutions for (29) on Figures 2–3 grids.

Grid	$\|Q_0u - u_0\|_0$	rate	$\|\nabla_w(Q_hu - u_h)\|_0$	rate	# iteration
	The $\{P_3, P_2\}$ WG element (4), by 4-subdomain iteration.				
1	0.366E-01	0.0	0.279E-01	0.0	10
2	0.236E-02	4.0	0.632E-02	2.1	12
3	0.151E-03	4.0	0.947E-03	2.7	16
4	0.947E-05	4.0	0.126E-03	2.9	25
5	0.592E-06	4.0	0.162E-04	3.0	44
	The $\{P_3, P_2\}$ WG element (4), by 16-subdomain iteration.				
1	0.366E-01	0.0	0.279E-01	0.0	10
2	0.236E-02	4.0	0.631E-02	2.1	14
3	0.151E-03	4.0	0.939E-03	2.7	19
4	0.946E-05	4.0	0.125E-03	2.9	35
5	0.592E-06	4.0	0.161E-04	3.0	59

3 that an order four convergence in the L^2-norm and an order three convergence in the energy norm are observed. Table 3 shows that the number of iterations for the 16-subdomain iteration is somewhat higher than that of the 4-subdomain iteration. Note that the two iterations are the same as there are only 4 squares on the first level grid.

The numerical results for the $\{P_4, P_3\}$, $\{P_5, P_4\}$ and $\{P_6, P_5\}$ WG finite element solutions by the 4-subdomain and 16-subdomain iterations are respectively listed in Tables 4-6 with corresponding $\beta = 32$, $\beta = 19$ and $\beta = 32$. In all these computations, we have observed the optimal order of convergence in the L^2-norm and the energy norm. It seems that larger β may reduce the number of iterations for higher order finite elements. It is surprising that 78-iteration shows up for the $\{P_4, P_3\}$-element with 4-subdomain iterations on the fifth-level grid. Another noticeable surprise is that the number of iterations for the 4-subdomain iteration increases much less than that of the 16-subdomain iteration, when the $\{P_5, P_4\}$ and $\{P_6, P_5\}$

TABLE 4. Error profile of $\{P_4, P_3\}$ solutions for (29) on Figures 2–3 grids.

Grid	$\|Q_0u - u_0\|_0$	rate	$\|\nabla_w(Q_hu - u_h)\|_0$	rate	# iteration
	By $\{P_4, P_3\}$ element (4), 4-subdomain iteration, $\beta = 32$.				
1	0.579E-02	0.0	0.123E-01	0.0	29
2	0.243E-03	4.6	0.114E-02	3.4	55
3	0.861E-05	4.8	0.802E-04	3.8	96
4	0.278E-06	5.0	0.522E-05	3.9	121
5	0.889E-08	5.0	0.331E-06	4.0	78
	By $\{P_4, P_3\}$ element (4), 16-subdomain iteration, $\beta = 32$.				
1	0.579E-02	0.0	0.123E-01	0.0	29
2	0.244E-03	4.6	0.115E-02	3.4	59
3	0.861E-05	4.8	0.802E-04	3.8	97
4	0.278E-06	5.0	0.522E-05	3.9	121
5	0.877E-08	5.0	0.331E-06	4.0	139

finite elements move to higher level grids. We conjecture that it might be due to non-hanging subdomains in the 4-subdomain iterations.

TABLE 5. Error profile of $\{P_5, P_4\}$ solutions for (29) on Figures 2–3 grids.

Grid	$\|Q_0u - u_0\|_0$	rate	$\|\nabla_w(Q_hu - u_h)\|_0$	rate	# iteration
	By $\{P_5, P_4\}$ element (4), 4-subdomain iteration, $\beta = 19$.				
1	0.146E-02	0.0	0.394E-02	0.0	31
2	0.357E-04	5.4	0.154E-03	4.7	55
3	0.621E-06	5.8	0.513E-05	4.9	71
4	0.996E-08	6.0	0.165E-06	5.0	78
	By $\{P_5, P_4\}$ element (4), 16-subdomain iteration, $\beta = 19$.				
1	0.146E-02	0.0	0.394E-02	0.0	31
2	0.357E-04	5.4	0.154E-03	4.7	59
3	0.621E-06	5.8	0.513E-05	4.9	81
4	0.996E-08	6.0	0.165E-06	5.0	104

TABLE 6. Error profile of $\{P_6, P_5\}$ solutions for (29) on Figures 2–3 grids.

Grid	$\|Q_0u - u_0\|_0$	rate	$\|\nabla_w(Q_hu - u_h)\|_0$	rate	# iteration
	By $\{P_6, P_5\}$ element (4), 4-subdomain iteration, $\beta = 32$.				
1	0.342E-03	0.0	0.711E-03	0.0	43
2	0.348E-05	6.6	0.129E-04	5.8	67
3	0.289E-07	6.9	0.211E-06	5.9	99
4	0.232E-09	7.0	0.337E-08	6.0	94
	By $\{P_6, P_5\}$ element (4), 16-subdomain iteration, $\beta = 32$.				
1	0.342E-03	0.0	0.711E-03	0.0	43
2	0.348E-05	6.6	0.129E-04	5.8	97
3	0.289E-07	6.9	0.211E-06	5.9	133
4	0.232E-09	7.0	0.334E-08	6.0	156

7.2. Test Example 2. We solve the elliptic boundary value model problem (1) where the configuration is set up as follows: $a(x, y) = 1$; $c = 0$; the exact solution

$$u(x, y) = 4(x - x^3)(y - y^3); \tag{30}$$

and the domain $\Omega = (0, 1)^2$. The polygonal grids of quadrilaterals and pentagons, shown as in Figures 4 and 5, are employed in this test. The 4-subdomain iterations and 16-subdomain iterations are computed respectively.

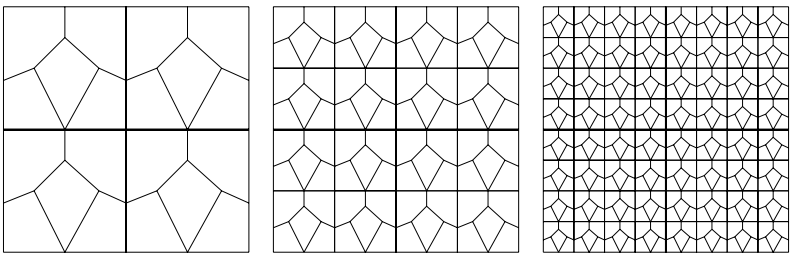

FIGURE 4. The first three levels of grids for the 4-subdomain iteration in Tables 7–8.

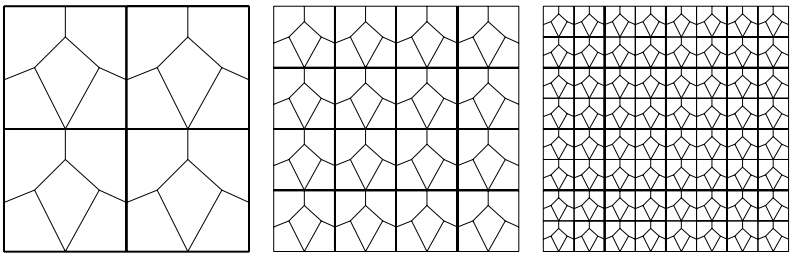

FIGURE 5. The first three levels of grids for the 16-subdomain iteration in Tables 7–8.

The computational results for the $\{P_2, P_1\}$ weak Galerkin finite element are listed in Table 7. Note that $Q_h u = \{Q_0 u, Q_b u\}$ where Q_0 is the element-wise L^2 projection to the space $P_k(T)$ and Q_b is the edge-wise L^2 projection to the space $P_{k-1}(e)$. In the computation, the iterative process is stopped when the iterative error achieves the truncation error. The numerical solution converges at the optimal order in the L^2-norm and in the energy norm respectively. The number of iterations for the 4-subdomain method is slightly less than that of the 16-subdomain method.

The errors for the $\{P_3, P_2\}$ and $\{P_4, P_3\}$ weak Galerkin finite elements (4) are listed in Table 8. The numerical solutions converge at the optimal order in the L^2-norm and in the energy norm respectively. Due to the use of polygonal meshes, the round-off error is accumulated to be very large for the computation of $\{P_4, P_3\}$ element on the 4th-level grid. We observe that for the high-order finite elements, the number of iteration may not increase when the number of the grid level increases.

TABLE 7. Error profile of $\{P_2, P_1\}$ (4) solutions on Figures 4–5 grids, and the number of iterations with 4-subdomains and 16-subdomains.

Grid	$\|Q_0u - u_0\|_0$	rate	$\|\nabla_w(Q_hu - u_h)\|_0$	rate	# iteration	
	The $\{P_2, P_1\}$ WG element				4-sub	16-sub
1	0.180E-01	0.0	0.817E-01	0.0	20	20
2	0.228E-02	3.0	0.202E-01	2.0	24	41
3	0.287E-03	3.0	0.491E-02	2.0	32	54
4	0.349E-04	3.0	0.121E-02	2.0	43	68
5	0.432E-05	3.0	0.299E-03	2.0	54	84
6	0.543E-06	3.0	0.745E-04	2.0	60	99

TABLE 8. Error profile of $\{P_k, P_{k-1}\}$ (4) solutions on Figures 4–5 grids, and the number of iterations with 4-subdomains and 16-subdomains.

Grid	$\|Q_0u - u_0\|_0$	rate	$\|\nabla_w(Q_hu - u_h)\|_0$	rate	# iteration	
	The $\{P_3, P_2\}$ WG element				4-sub	16-sub
1	0.174E-02	0.0	0.933E-02	0.0	39	39
2	0.110E-03	4.0	0.126E-02	2.9	51	55
3	0.687E-05	4.0	0.162E-03	3.0	84	89
4	0.438E-06	4.0	0.207E-04	3.0	59	86
5	0.278E-07	4.0	0.260E-05	3.0	69	115
	The $\{P_4, P_3\}$ WG element				4-sub	16-sub
1	0.115E-03	0.0	0.417E-03	0.0	44	44
2	0.364E-05	5.0	0.274E-04	3.9	64	64
3	0.114E-06	5.0	0.176E-05	4.0	99	93
4	0.469E-08	—	0.113E-06	4.0	95	111

7.3. Test Example 3. We shall test the subdomain iterations for a superconvergent WG finite element method [37]. We consider the Poisson equation on the domain $\Omega = (0,1)^2$ with the exact solution $u(x,y) = \sin(\pi x)\sin(\pi y)$. The superconvergent $\{P_k, P_k\}$ WG finite element was introduced in [37] as follows:

$$\{\{v_0, v_b\} : v_0 \in P_k(T),\ v_b \in P_k(e),\ e \subset T,\ T \in \mathcal{T}_h\}. \tag{31}$$

For this superconvergent $\{P_k, P_k\}$ WG finite element, the weak gradient is defined by $\nabla_w v_h \in \mathrm{R}\underline{\mathrm{T}}_k = P_k(T)^2 + \underline{\mathrm{x}}P_k(T)$, satisfying

$$(\nabla_w v_h, \underline{\mathrm{q}})_T = -(v_0, \operatorname{div}\underline{\mathrm{q}})_T + \langle v_b, \underline{\mathrm{q}}\cdot\underline{\mathrm{n}}_T\rangle_{\partial T}, \quad \forall \underline{\mathrm{q}} \in \mathrm{R}\underline{\mathrm{T}}_k. \tag{32}$$

For this WG finite element, the stabilizer $s(\cdot,\cdot)$ is dropped from the WG scheme (8), in order to get one-order superconvergence as discussed in [37].

We take $\beta = 4$ in all $\{P_k, P_k\}$ weak Galerkin finite element computations. Note that $Q_hu = \{Q_0u, Q_bu\}$ where Q_0u is the triangle-wise L^2 projection of u onto the polynomial space $P_k(T)$ and Q_b is the edge-wise L^2 projection of u onto the polynomial space $P_k(e)$. Again the iteration is stopped when the iterative error is about the truncation error. In Tables 9-12, we have observed one-order superconvergence for the $\{P_k, P_k\}$ weak Galerkin finite element defined in (31), in both the L^2-norm and the energy norm.

TABLE 9. Error profile for the $\{P_1, P_1\}$ solution on Figures 2–3 grids.

Grid	$\|Q_0u - u_0\|_0$	rate	$\|\nabla_w(Q_hu - u_h)\|_0$	rate	# iteration
	The $\{P_1, P_1\}$ WG element (31), by 4-subdomain iteration.				
1	0.208E-01	0.0	0.500E+00	0.0	7
2	0.305E-02	2.8	0.140E+00	1.8	9
3	0.393E-03	3.0	0.362E-01	2.0	13
4	0.494E-04	3.0	0.912E-02	2.0	12
5	0.624E-05	3.0	0.229E-02	2.0	17
6	0.789E-06	3.0	0.572E-03	2.0	26
7	0.994E-07	3.0	0.143E-03	2.0	42
	The $\{P_1, P_1\}$ WG element (31), by 16-subdomain iteration.				
1	0.208E-01	0.0	0.500E+00	0.0	9
2	0.304E-02	2.8	0.140E+00	1.8	11
3	0.392E-03	3.0	0.362E-01	2.0	13
4	0.496E-04	3.0	0.913E-02	2.0	13
5	0.631E-05	3.0	0.229E-02	2.0	18
6	0.795E-06	3.0	0.572E-03	2.0	30
7	0.101E-06	3.0	0.143E-03	2.0	48

TABLE 10. Error profile for the $\{P_2, P_2\}$ solution on Figures 2–3 grids.

Grid	$\|Q_0u - u_0\|_0$	rate	$\|\nabla_w(Q_hu - u_h)\|_0$	rate	# iteration
	The $\{P_2, P_2\}$ WG element (31), by 4-subdomain iteration.				
1	0.320E-02	0.0	0.116E+00	0.0	12
2	0.203E-03	4.0	0.158E-01	2.9	12
3	0.127E-04	4.0	0.202E-02	3.0	14
4	0.802E-06	4.0	0.254E-03	3.0	25
5	0.507E-07	4.0	0.318E-04	3.0	48
6	0.321E-08	4.0	0.398E-05	3.0	92
	The $\{P_2, P_2\}$ WG element (31), by 16-subdomain iteration.				
1	0.320E-02	0.0	0.116E+00	0.0	16
2	0.202E-03	4.0	0.158E-01	2.9	12
3	0.128E-04	4.0	0.202E-02	3.0	15
4	0.801E-06	4.0	0.254E-03	3.0	29
5	0.508E-07	4.0	0.318E-04	3.0	55
6	0.321E-08	4.0	0.398E-05	3.0	107

As expected, the number of 16-subdomain iterations would be more than that of 4-subdomain iterations for the $\{P_1, P_1\}$ weak Galerkin finite element as we can see from Table 9.

In Table 10, we list the computational results for the $\{P_2, P_2\}$ weak Galerkin finite element. Worse than the $\{P_1, P_1\}$ computation, the number of iterations for 16-subdomains is much more than that of 4-subdomain. But on the other side, a better parallelization is possible for the computation with 16-subdomains.

Table 11 shows that the number of iterations for 16-subdomains is about the same as that of 4-subdomains for the $\{P_3, P_3\}$ weak Galerkin finite element.

TABLE 11. Error profile for the $\{P_3, P_3\}$ solution on Figures 2–3 grids.

Grid	$\|Q_0u - u_0\|_0$	rate	$\|\nabla_w(Q_hu - u_h)\|_0$	rate	# iteration
	The $\{P_3, P_3\}$ WG element (31), by 4-subdomain iteration.				
1	0.478E-03	0.0	0.222E-01	0.0	12
2	0.179E-04	4.7	0.149E-02	3.9	24
3	0.593E-06	4.9	0.944E-04	4.0	44
4	0.189E-07	5.0	0.593E-05	4.0	82
5	0.597E-09	5.0	0.372E-06	4.0	142
	The $\{P_3, P_3\}$ WG element (31), by 16-subdomain iteration.				
1	0.478E-03	0.0	0.222E-01	0.0	12
2	0.179E-04	4.7	0.149E-02	3.9	22
3	0.593E-06	4.9	0.944E-04	4.0	46
4	0.189E-07	5.0	0.593E-05	4.0	80
5	0.596E-09	5.0	0.372E-06	4.0	161

TABLE 12. Error profiles for the P_4,P_5 and P_6 WG solution on Figures 2–3 grids.

Grid	$\|Q_0u - u_0\|_0$	rate	$\|\nabla_w(Q_hu - u_h)\|_0$	rate	# iteration
	The $\{P_4, P_4\}$ WG element (31), by 4-subdomain iteration.				
2	0.120E-05	6.0	0.122E-03	4.9	34
3	0.190E-07	6.0	0.388E-05	5.0	54
4	0.301E-09	6.0	0.122E-06	5.0	123
	The $\{P_4, P_4\}$ WG element (31), by 16-subdomain iteration.				
2	0.119E-05	6.0	0.122E-03	4.9	24
3	0.190E-07	6.0	0.387E-05	5.0	62
4	0.300E-09	6.0	0.123E-06	5.0	133
	The $\{P_5, P_5\}$ WG element (31), by 4-subdomain iteration.				
1	0.938E-05	0.0	0.541E-03	0.0	18
2	0.827E-07	6.8	0.896E-05	5.9	36
3	0.655E-09	7.0	0.141E-06	6.0	95
	The $\{P_5, P_5\}$ WG element (31), by 16-subdomain iteration.				
1	0.938E-05	0.0	0.541E-03	0.0	18
2	0.816E-07	6.8	0.890E-05	5.9	44
3	0.647E-09	7.0	0.141E-06	6.0	111
	The $\{P_6, P_6\}$ WG element (31), by 4-subdomain iteration.				
1	0.115E-05	0.0	0.710E-04	0.0	24
2	0.460E-08	8.0	0.579E-06	6.9	66
3	0.185E-10	8.0	0.459E-08	7.0	162
	The $\{P_6, P_6\}$ WG element (31), by 16-subdomain iteration.				
1	0.115E-05	0.0	0.710E-04	0.0	24
2	0.459E-08	8.0	0.578E-06	6.9	72
3	0.185E-10	8.0	0.461E-08	7.0	166

Finally the computational results by using $\{P_4, P_4\}$, $\{P_5, P_5\}$, $\{P_6, P_6\}$ weak Galerkin finite elements are illustrated in Table 12. In all these cases, the number of 16-subdomain iterations is slightly bigger than that of the 4-subdomain iterations.

8. Conclusion

In conclusion, this paper has introduced and examined a parallelizable iterative procedure that hinges on domain decomposition. The focal point of this procedure is its application in tandem with weak Galerkin finite element methods for second order elliptic equations. The conducted convergence analysis has illuminated the efficacy of domain decomposition, whether executed on individual elements associated with weak Galerkin methods or on larger subdomains. The viability of the proposed approach has been substantiated through a comprehensive array of numerical tests. This empirical validation serves to corroborate the theoretical framework articulated within this paper. Overall, the amalgamation of theoretical insights and practical confirmation underscores the potential of the parallelizable iterative procedure and its relevance in advancing the realm of numerical solutions for elliptic equations.

Acknowledgements

The research of Chunmei Wang was partially supported by National Science Foundation Award DMS-2136380. The research of Junping Wang was supported in part by the NSF IR/D program, while working at National Science Foundation. However, any opinion, finding, and conclusions or recommendations expressed in this material are those of the author and do not necessarily reflect the views of the National Science Foundation.

References

[1] D. Arnold, and F. Brezzi, Mixed and nonconforming finite element methods: implementation, postprocessing and error estimates, R.A.I.R.O., Modelisation Math. Anal. Numer. 19, 7-32, 1985.

[2] F. Brezzi, Jr. Douglas, M. Marini, Efficient rectangular mixed finite elements in two and three space variables, R.A.I.R.O., Modelisation Math. Anal. Numer. 21, 581-604, 1987.

[3] F. Brezzi, Jr. Douglas, M. Marini, Two families of mixed finite elements for second order elliptic problems, Numer. Math. 47, 217-235, 1985.

[4] F. Brezzi, Jr. Douglas, R. Duran, M. Fortin, Mixed finite elements for second order elliptic problems in three variables, Numer. Math. 51, 237-250, 1987.

[5] L. Chen, J. Wang, Y. Wang and X. Ye, An auxiliary space multigrid preconditioner for the weak Galerkin method, Comput. Math. Appl. 70(4), pp. 330-344, 2015.

[6] B. Despres, Methodes de decomposition de domains pour les problems de propagation d'ondes en regime harmonique, these, Univeristy Paris IX Dauphine, UER, Mathematiques de la Decision, 1991.

[7] B. Despres, Domain decomposition and the Helmholz problem, Proceedings of First International conference on Mathematical and Numerical Aspects of Wave Propagation.

[8] B. Despres, P. Joly and J. E. Roberts, Domain decomposition method for harmonic Maxwell's equations, Proceedings of the IMACS international symposium on iterative methods in linear algebra, Elsevier, North Holland, 1990.

[9] Jr. Douglas, P.J. Leme, J. E. Roberts and J. Wang, A parallel iterative procedure applicable to the approximate solution of second order partial differential equations by mixed finite element methods, Numer. Math., 65, 95-108, 1993.

[10] B. X. Fraeijs de Veubeke , Displacement and equilibrium models in the finite element method, In: O. C. Zienkiewicz, G. Holister, eds, Stress Analysis, Wiley, New York, 1965.

[11] B . X. Fraeijs de Veubeke, Stress function approach, International Congress on the finite element method in structural mechanics, Bournemouth, 1975.

[12] V. Ginting, G. Lin and J. Liu, On application of the weak Galerkin finite element method to a two-phase model for subsurface flow, J. Sci. Comput., 66 (2016), pp. 225-239.

[13] P. Jolivet, F. Hecht, F. Nataf and C. PrudHomme, Scalable domain decomposition preconditioners for heterogeneous elliptic problems, Sci. Programming 22 (2014), pp. 157-171.

[14] B. Li, X. Xie and S. Zhang, BPS preconditioners for a weak Galerkin finite element method for 2D diffusion problems with strongly discontinuous coefficients, Comput. Math. Appl. 76(4), pp.701-724, 2018.
[15] L. Mu, J. Wang, Y. Wang, and X. Ye, A computational study of the weak Galerkin method for second-order elliptic equations, Numer. Algor., 63(2012), pp. 753-777.
[16] L. Mu, J. Wang, G. Wei, X. Ye, and S. Zhao, Weak Galerkin methods for second order elliptic interface problems, J. Comput. Phys., 250(2013), pp.106-125.
[17] L. Mu, J. Wang, and X. Ye, Weak Galerkin finite element methods for the biharmonic equation on polytopal meshes, Numer. Methods Partial Differential Equations, 30(3)(2014), pp. 1003-1029.
[18] L. Mu, J. Wang, and X. Ye, Weak Galerkin finite element method for second-order elliptic problems on polytopal meshes, Int. J. Numer. Anal. Mod. 12(2015), pp. 31-53.
[19] L. Mu, J. Wang, and X. Ye, A weak Galerkin finite element method with polynomial reduction, J. Comput. Appl. Math. 285 (2015), pp. 45-58.
[20] L. Mu, J. Wang, X. Ye, and S. Zhang, A C^0-weak Galerkin finite element method for the biharmonic equation, J. Sci. Comput. 59(2014), pp. 473-495.
[21] F. Qin, M. Zha and F. Wang, A two-level additive Schwarz preconditioning algorithm for the weak Galerkin method for the second-order elliptic equation, Math. Probl. Eng. 2016.
[22] X. Tu and B. Wang, A BDDC Algorithm for Weak Galerkin Discretizations, In Domain Decomposition Methods in Science and Engineering XXIII (pp. 269-276), Springer International Publishing, 2017.
[23] X. Tu and B. Wang, A BDDC algorithm for the Stokes problem with weak Galerkin discretizations, Comput. Math. Appl. 76(2018), pp. 377-392.
[24] Z. Wang, G. Harper, P. O'Leary, J. Liu and S. Tavener, deal.II implementation of a weak Galerkin finite element solver for Darcy flow, Lec. Notes Comput. Sci., 11539 (2019), pp. 495-509.
[25] C. Wang and J. Wang, A Hybridized Formulation for Weak Galerkin Finite Element Methods for Biharmonic Equation on Polygonal or Polyhedral Meshes, Int. J. Numer. Anal. Mod. 12 (2015), pp. 302-317.
[26] C. Wang, and J. Wang, An efficient numerical scheme for the biharmonic equation by weak Galerkin finite element methods on polygonal or polyhedral meshes, J. Comput. Math. Appl. 68(2014), pp. 2314-2330.
[27] C. Wang, and J. Wang, A hybridized formulation for weak Galerkin finite element methods for biharmonic equation on polygonal or polyhedral meshes, Int. J. Numer. Anal. Mod., 12(2015), pp. 302-317.
[28] J. Wang, and C. Wang, Weak Galerkin finite element methods for elliptic PDEs, Science China, 45(2015), pp. 1061-1092.
[29] C. Wang, and J. Wang, Discretization of div-curl systems by weak Galerkin finite element methods on polyhedral partitions, J. Sci. Comput., 68 (2016), 1144-1171.
[30] C. Wang, and J. Wang, A primal-dual weak Galerkin finite element method for second order elliptic equations in non-divergence form, Math. Comp., 87 (2018), 515-545.
[31] C. Wang, J. Wang, R. Wang, and R. Zhang, A locking-free weak Galerkin finite element method for elasticity problems in the primal formulation, J. Comput. Appl. Math., 307(2016), pp. 346-366.
[32] C. Wang, J. Wang, X. Ye, and S. Zhang, De Rham Complexes for Weak Galerkin Finite Element Spaces, J. Comput. Appl. Math., vol. 397, pp. 113645, 2021.
[33] J. Wang, and X. Ye, A weak Galerkin finite element method for second-order elliptic problems, J. Comp. and Appl. Math., 241(2011), pp. 103-115.
[34] J. Wang, and X. Ye, A weak Galerkin mixed finite element method for second-order elliptic problems, Math. Comp., vol. 83, pp. 2101-2126, 2014.
[35] J. Wang, and X. Ye, A weak Galerkin finite element method for the Stokes equations, Adv. Comput. Math., 42(2016), pp. 155-174.
[36] C. Wang, and H. Zhou, A weak Galerkin finite element method for a type of fourth order problem arising from fluorescence tomography, J. Sci. Comput., 71(3)(2017), pp. 897-918.
[37] X. Ye and S. Zhang, A stablizer free weak Galerkin finite element method on polytopal mesh: part II, J. Comput. Appl. Math. 394 (2021), Paper No. 113525, 11 pp.

Department of Mathematics, University of Florida, Gainesville, FL 32611, USA
E-mail: chunmei.wang@ufl.edu

Division of Mathematical Sciences, National Science Foundation, Alexandria, VA 22314, USA
E-mail: jwang@nsf.gov

Department of Mathematical Sciences, University of Delaware, Newark, DE 19716, USA
E-mail: szhang@udel.edu